Dendritic Spherical Polymer Brushes: Theory and Self-Consistent Field Modeling

ARTICLE *in* MACROMOLECULES · MAY 2013

Impact Factor: 5.8 · DOI: 10.1021/ma302632b

7 AUTHORS, INCLUDING:

Alexey A. Polotsky
Russian Academy of Sciences
46 PUBLICATIONS **345** CITATIONS
SEE PROFILE

Frans A M Leermakers
Wageningen University
288 PUBLICATIONS **4,741** CITATIONS
SEE PROFILE

Marcus Textor
ETH Zurich
333 PUBLICATIONS **13,999** CITATIONS
SEE PROFILE

T.M. Birshtein
Russian Academy of Sciences
240 PUBLICATIONS **3,486** CITATIONS
SEE PROFILE

Macromolecules

Article

pubs.acs.org/Macromolecules

Dendritic Spherical Polymer Brushes: Theory and Self-Consistent Field Modeling

Oleg V. Rud,*[,†,&] Alexey A. Polotsky,[†] Torben Gillich,[‡] Oleg V. Borisov,*[,§] Frans A. M. Leermakers,[∥] Marcus Textor,[‡] and Tatiana M. Birshtein[†]

[†]Institute of Macromolecular Compounds, Russian Academy of Sciences, Laboratory of Theory and Simulation of Polymer Systems, Saint-Petersburg, Russia

[‡]Laboratory for Surface Science and Technology, ETH, Zurich, Switzerland

[§]IPREM UMR 5254 CNRS/UPPA, Pau, France

[∥]Laboratory of Physical Chemistry and Colloid Science, Wageningen University, Wageningen, The Netherlands

[⊥]Facility of Physics, St. Petersburg State University, Saint-Petersburg, Russia

[&]Laboratory of Physics, Lappeenranta University of Technology, Box 20, 53851 Lappeenranta, Finland

ABSTRACT: Equilibrium structural properties of polymer brushes formed by dendrons grafted via the root segment onto spherical surfaces (dendritic spherical polymer brushes, DSPB) are studied by means of the Scheutjens−Fleer self-consistent field (SF-SCF) numerical approach and scaling analysis. In particular, we focus on the effects of the variable curvature of the surface on the polymer volume fraction distribution and extension of the individual dendrons in DSPB. A systematic comparison with spherical polymer brushes formed by linear polymer chains (LSPB) end-grafted to the surfaces of the same curvature radii is performed. We demonstrate that the difference in internal structural organization of DSPB and LSPB is most pronounced at small curvature radius of the grafting surface. In particular, the radial distribution of polymer volume fraction in DSPB is close to uniform, whereas in LSPB it decays in the radial direction following a power law. The quasi-plateau polymer volume fraction distribution in DSPB is ensured by wide radial distribution of the end segments. In contrast, in LSPB the end segments of the chains are localized preferentially close to the periphery of the brush. An increase in the curvature radius of the surface is accompanied by emerging segregation into two (or more, for larger number of generations) populations of dendrons: the less extended and the more extended ones. The former ones fill the space in the central region of the DSPB, and the latter bring the majority of the monomer units closer to the periphery of the DSPB. The theoretical results are in line with experimental findings on hydrodynamic radii of linear and dendritic poly(ethylene glycol) brushes end-grafted onto Fe_3O_4 nanoparticles.

1. INTRODUCTION

Dendritic polymer brushes, that is, monolayers formed by regularly branched macromolecules ("dendrons") grafted onto the surface and immersed in a solvent (Figure 1), have recently come into the focus of theoretical studies.[1−7] This interest was initiated by advances in grafting of oligo(ethylene glycol)-based dendrons with well-controlled number of generations and variable length of oligo(ethylene glycol) (OEG) spacers onto various metal oxide surfaces. Grafting of OEG-based dendrons onto the surface was achieved by using dendrons with catechol surface-reactive root segments (focal points) with multiple dihydroxyphenylalanine, DOPA, or single nitrocatechol anchors.[8,9] The experimental activity was motivated, first of all, by possible application of the dendritic PEG brushes for creating "antifouling" surfaces that resist to nonspecific protein adsorption. Moreover, a large number of exposed to the external solution end groups in dendritic molecules attached to the surface enable one to specifically functionalize them for tuning selective biological response of the surface, which is crucially important for a wide range of biomedical applications (medical devices such as implants, diagnostics assays, etc.).

Progress both in experimental characterization and in theoretical understanding of structure and specific conformational properties of dendritic polymer brushes on planar two-

Received: December 23, 2012
Revised: April 9, 2013
Published: May 21, 2013

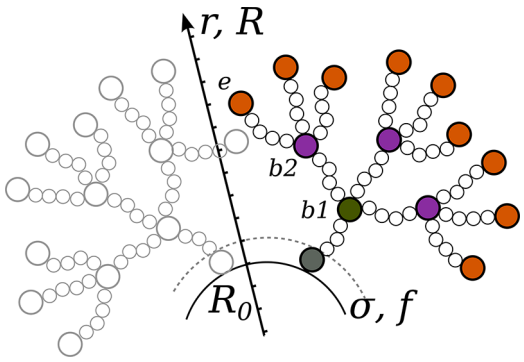

Figure 1. Schematic illustration of spherical brush composed of f dendrons, grafted with a density σ. Each dendron has functionality q = 3, spacer length n = 5, and number of generations g = 2. The monomer units corresponding to the branching points (prefix b) are denoted as $b1$ and $b2$ for the first and the second generations, respectively, whereas the terminal monomer units are denoted as e. Here R is the distance from the center of curvature, and $r = R - R_0$ is the distance from the grafting surface.

dimensional surfaces has recently been achieved. The feasibility to reach high polymer volume fraction in the dendritic brush enables to achieve excellent protein-resistant properties even at much lower thickness of the brush when compared to conventional linear chain brushes of comparable molecular weight.

Detailed theoretical studies of internal structure of dendritic polymer brushes grafted onto planar surfaces have been performed by means of the Scheutjens–Fleer self-consistent field (SF-SCF) approach.[3,5] A principal result of this study was the demonstration that at sufficiently high grafting density dendrons are divided into populations differing in the degree of stretching. All together, the large-scale fluctuations in the extension of individual dendrons ensure quasi-plateau polymer volume fraction profile in the direction perpendicular to the surface. In the particular case of the brush formed by the first generation dendrons (equivalent to the brush formed by star-shaped polymers attached to the surface by the end segment of one of the arms), one finds two populations of dendrons: the less extended ones contribute mostly to the polymer volume fraction close to the grafting surface (central region of the brush) whereas the more extended ones reach the periphery and "fill" by their monomer units the regions close to the edge of the brush.[3,5] These predictions of the SCF theory for brushes formed by arm-grafted stars were also confirmed by molecular dynamics simulations.[4]

Colloidal or spherical polymer brushes formed by linear polymer chains (LSPB) end-grafted to the spherical "core" nanoparticles were amply studied in past decade (see ref 10 for a comprehensive review). Nonionic, polyelectrolyte, and even zwitterionic LSPB were synthesized; their stimuli-responsive properties in terms of conformational changes triggered by variation in external conditions have been demonstrated.

Functionalization of the nanoparticle surface by end-grafted linear PEG chains has been demonstrated to have an impact on colloidal (aggregative) stability combined with stealth properties ("nonfouling") of the particles. The steric repulsions arising between sufficiently dense and highly hydrated PEG coronae is strong enough to overcome van der Waals attraction between the Fe_3O_4 particles, thus preventing their aggregation. Key aspects of nanoparticle stability, particularly if they are ultrasmall (less than 10 nm in diameter), are a high density of the polymer chains (higher than for nonfouling two-dimensional surfaces) and, directly correlated, a strong surface anchor with an adhesion energy that is able to overcome the high interchain repulsions within the polymer shell.[8,9] The stabilizing properties of the linear chain PEG corona were furthermore found to depend on the PEG chain length (optimal range is 2–10 kDa) as well as on temperature, since PEG exhibits a LCST transition[11] close to 100 °C depending on molecular weight and ionic strength of the medium.

A theoretical understanding of the chain conformations in LSPB[12−15] was achieved on the basis of classical scaling models.[16−19] It was demonstrated that steric repulsions acting between crowded chains in the LSPB under good or theta-solvent conditions give rise to the chain extension in the radial direction. If the curvature radius of the grafting surface R_0 is significantly smaller than characteristic dimensions of the macromolecular chains, the LSPB resembles a star-branched macromolecule. In this limit the polymer volume fraction $c(R)$ in the LSPB as well as local stretching of the chains decay as power-law functions of the radial distance $R > R_0$ from the center of the sphere, with the exponents dependent on the solvent strength.

The numerical SCF calculations[20,21] have demonstrated that under good and theta-solvent strength conditions the radial distribution of the end segments of the chains in LSPB with a small core exhibits a pronounced peak at the periphery of the brush, whereas in the proximal to the core region no end segments are found. Hence, the equal stretching approximation is sufficiently accurate for starlike LSPB. In contrast, internal structure of weakly curved LSPB is close to the structure of planar polymer brushes. The latter is characterized by essentially nonpower law radial decay of the polymer volume fraction and distribution of the end segments throughout the brush thickness.[22−25]

Recently, the catechol-based anchorage concept was successfully applied for end grafting of OEG dendrons to spherical superparamagnetic nanoparticles (SPIONs) with a diameter of about 7 nm. SPIONs found a number of applications, notably as contrast agent in magnetic resonance imaging (MRI). The use of dendritic instead of linear PEG chains for surface modification is motivated by a promise to achieve better stabilizing properties and thus better performance of the PEG-functionalized nanoparticles of similar stability but with thinner polymer shells. This may be crucial for applications where the size of the particles is the key to performance such as the ability to cross biological barriers in biomedical applications.

The internal structural organization and, consequently, the elastic properties of the dendritic spherical polymer brushes (DSPB) are expected to differ significantly from those of LSPB formed by linear polymer chains. The aim of the present study is to compare systematically structural properties of polymer brushes formed by dendritic versus linear polymer chains end-grafted to spherical surface of variable curvature radius.

The paper is organized as follows. We start with discussing a theoretical model of a brush formed by dendrons grafted by the root segment to the surface of a spherical core particle (section 2). In section 3 we present a simple Flory-like approach targeted to describe the structure of a dendritic brush. Here the focus is on limiting cases of minimal and maximal possible losses of conformational entropy that result from different assumptions with respect to the distribution of the elastic tension in end-grafted dendrons. In section 4 we present a

dx.doi.org/10.1021/ma302632b | Macromolecules 2013, 46, 4651–4662

detailed comparative analysis of the structural organization of brushes formed by dendrons and by linear polymers grafted onto spherical particles. In section 5 we outline the most important theoretical predictions and compare them to the results obtained for experimental systems consisting of oligo(ethylene glycol) (OEG) dendrons of the second generation or of linear OEG molecules of approximately the same molecular weight grafted to the Fe_3O_4 superparamagnetic nanoparticles through a catechol-based anchor group. Finally, we sum up our conclusions.

2. THEORETICAL MODEL OF THE DSPB

Consider a DSPB formed by dendrons grafted by the terminal (root) segment onto the surface of a spherical core particle of radius R_0 and immersed in a solvent (Figure 1). The surface area of the core per dendron is s; that is, $\sigma = 1/s$ is grafting density of the dendrons. Hence, the total number of end-grafted dendrons in the DSPB is $f = 4\pi R_0^2\sigma$. We assume that the distance, $s^{1/2}$, between two neighboring dendrons is smaller than the characteristic size of an individual dendron under the same solvent strength conditions.

A dendron is characterized by the number of generations g and a functionality $q = 2, 3, \ldots$ of each branching point. The functionality is defined as the ratio between the number of spacers in generation $g + 1$ and that in generation g. The number of monomer units per spacer, n, is fixed throughout the dendron. We assume (and this corresponds to the reference experimental system comprising dendrons with flexible PEO spacers[8,9]) that the spacers in the dendrons are intrinsically flexible. That is, the statistical segment length is on the order of monomer unit size a. Below we use a as the unit length.

The number of monomer units in a dendron of generation $g = 0, 1, 2, \ldots$ equals

$$N = n(q^{g+1} - 1)/(q - 1) \tag{1}$$

The total number of monomer units in the DSPB is Nf. The dendrons of the zeroth generation ($g = 0$) or the dendrons with $q = 1$ are simple linear chains. Hence, the DSPB formed by the dendrons with $g = 0$ or $q = 1$ is equivalent to the LSPB, which in the limit of small core radius resembles f-arm star polymer. In the limit of $R_0 \simeq 1$ a starlike DSPB with arbitrary g and q resembles a dendritically branched or "starburst" macromolecule.[26−30]

One can also introduce the number of monomer units in the longest path from the root of the dendron to any of its terminal points. This path includes one spacer from each generation and comprises

$$\mathcal{N} = n(g + 1) \tag{2}$$

monomer units. The ratio $N/\mathcal{N} = (q^{g+1} - 1)/[(q - 1)(g + 1)]$ does not depend on n and grows with an increase in both q and g. This ratio can be considered as a measure of the degree of branching in the dendrons. Obviously, for the linear chain ($g = 0$ or $q = 1$) $\mathcal{N} = N$.

Figure 1 shows the designation of "key" monomer units in a dendron: The monomer units corresponding to the first and the second branching points are denoted as $b1$ and $b2$, respectively, Here in the article we name all the key monomers of the same generation equally; the terminal monomer units are denoted as e.

3. SCALING THEORY OF DSPB

3.1. Free Energy of a Dendron in the Brush.

Conformations of dendrons in DSPB are controlled by the balance between steric (excluded volume) repulsions and conformational entropy penalty for the extension of branches. The free energy of a dendron in the DSPB can be presented as

$$F(H) = F_{int}(H) + F_{conf}(H) \tag{3}$$

where H is the characteristic size of a dendron in the direction perpendicular to the surface. The first term in (3) describes the free energy contribution due to (repulsive) excluded-volume interactions in the brush.

$$\frac{F_{int}}{k_BT} \cong N(vc + wc^2) \simeq \begin{cases} Nvc, & \text{good solvent} \\ Nwc^2, & \theta\text{-solvent} \end{cases} \tag{4}$$

where v and w are dimensionless the second and the third virial coefficients, respectively (the former characterizes the solvent strength and is related to the Flory−Huggins interaction parameter χ as $v = 1/2 - \chi$) and

$$c = \frac{3}{4\pi}\frac{Nf}{(R_0 + H)^3 - R_0^3} \simeq \begin{cases} \dfrac{N\sigma}{H}, & R_0 \gg H \\ \dfrac{3}{4\pi}\dfrac{Nf}{H^3}, & R_0 \ll H \end{cases} \tag{5}$$

is the average volume fraction of the monomer units in the DSPB. On the rhs of (5) two approximate expressions for c are given for the cases of a weakly curved (practically flat) DSPB, when $R_0 \gg H$, and a starlike DSPB, when $R_0 \ll H$.

To derive scaling (power law) relation between molecular weight (or the number of generations) and the thickness of the DSPB, however, certain *a priori* assumptions about the distribution of elastic tension within the dendrons should be made. Two possible limiting scenarios of radial stretching of the dendrons leading to two different functional forms for the $F_{conf}(H)$ can be envisioned.[3] The first one corresponds to the stretching of only one (arbitrary) longest elastic part within each dendron, whereas the spacers not belonging to this path remain unstretched. This scenario corresponds to minimal entropic penalty at given (average) radial extension of the dendrons:

$$\frac{F_{conf}^{(min)}}{k_BT} \cong \frac{H^2}{\mathcal{N}} \tag{6}$$

The opposite limiting scenario assumes that all the elastic paths in the dendron are uniformly stretched and leads to the maximal estimate of the conformational entropy losses at given size of the dendron.

$$\frac{F_{conf}^{(max)}}{k_BT} \cong \frac{H^2N}{\mathcal{N}^2} \tag{7}$$

Hence, the elastic contribution to the free energy, (6) and (7), can be presented in the general form

$$\frac{F_{conf}}{k_BT} \cong \frac{H^2}{N}\left(\frac{N}{\mathcal{N}}\right)^{\beta} \tag{8}$$

where the exponents $\beta = 1$ and $\beta = 2$ correspond to minimal and maximal estimates for the conformational entropy losses, respectively.

dx.doi.org/10.1021/ma302632b | Macromolecules 2013, 46, 4651−4662

Remarkably, at large degree of branching, $N/\mathcal{N} \gg 1$, that is the case for dendrons with large number of generations, the difference in entropic penalty for stretching in two described scenarios is significant. The presented below results of numerical SCF analysis of the structural properties of dendritic polymer brushes will allow us to evaluate the apparent exponent β and thus to get a valuable insight concerning the distribution of elastic tension in the dendrons forming the brush.

By using (5), the latter equation (8) can be rewritten in terms of average polymer volume fraction inside the brush

$$\frac{F_{\mathrm{conf}}}{k_{\mathrm{B}}T} = N\frac{\sigma^2}{c^2}\left(\frac{N}{\mathcal{N}}\right)^{\beta} \tag{9}$$

for quasi-planar case ($R_0 \gg H$) and

$$\frac{F_{\mathrm{conf}}}{k_{\mathrm{B}}T} = N\left(\frac{f}{N^2}\right)^{2/3} c^{-2/3}\left(\frac{N}{\mathcal{N}}\right)^{\beta} \tag{10}$$

for the starlike case ($R_0 \ll H$).

3.2. Scaling Relations. Balancing conformational entropy losses given by (9) or (10) with the free energy of repulsive interactions (4) enables one to derive the limiting power law expressions for the average volume fraction of monomer units in DSPB under good (index "+") and θ-solvent (index "θ") conditions:

$$c_+ \cong \left(\frac{v}{2}\right)^{-1/3}\sigma^{2/3}\left(\frac{N}{\mathcal{N}}\right)^{\beta/3}$$

$$c_\theta \cong w^{-1/4}\sigma^{1/2}\left(\frac{N}{\mathcal{N}}\right)^{\beta/4} \tag{11}$$

for quasi-planar ($R_0 \gg H$) and

$$c_+ \cong \left(\frac{2}{3v}\right)^{3/5}\left(\frac{f}{N^2}\right)^{2/5}\left(\frac{N}{\mathcal{N}}\right)^{3\beta/5}$$

$$c_\theta \cong \left(\frac{1}{3w}\right)^{3/8}\left(\frac{f}{N^2}\right)^{1/4}\left(\frac{N}{\mathcal{N}}\right)^{3\beta/8} \tag{12}$$

for starlike ($R_0 \ll H$) brush.

Each of the obtained relations (11) and (12), include two scaling parameters, one of these parameters refers to the brush as a whole, whereas the other one is characteristic for individual dendrons. The characteristic property of the planar brush is the grafting density σ. The characteristic property of the spherical brush is the ratio f/N^2. Each individual dendron is characterized by the degree of branching, $N/\mathcal{N}$.

By substituting the values of $\beta = 1$ or $\beta = 2$ into (11) and (12), one obtains the limiting estimates of polymer volume fraction in the brush corresponding to minimal and maximal entropy losses upon stretching of the dendrons, respectively. These values correspond to maximal and minimal limits for the brush height H.

In the limiting case of a quasi-planar dendritic brush, $R_0 \gg H$, the scaling dependences for the brush height derived in ref 3 are recovered:

$$H_+ \cong N\sigma^{1/3}v^{1/3}\left(\frac{N}{\mathcal{N}}\right)^{-\beta/3}$$

$$H_\theta \cong N\sigma^{1/2}w^{1/4}\left(\frac{N}{\mathcal{N}}\right)^{-\beta/4} \tag{13}$$

In the case of strongly curved DSPB, $R_0 \ll H$, we obtain

$$H_+ \cong N^{3/5}(fv)^{1/5}\left(\frac{N}{\mathcal{N}}\right)^{-\beta/5}$$

$$H_\theta \cong N^{1/2}(f^2w)^{1/8}\left(\frac{N}{\mathcal{N}}\right)^{-\beta/8} \tag{14}$$

Comparison of eqs 14 and 13 indicates that (i) the exponents of the power law dependences of H on N point to stronger extension of the dendrons in quasi-planar rather than in strongly curved brushes and (ii) the dependence of the brush thickness on the degree of branching $N/\mathcal{N}$ also becomes stronger upon an increase in the curvature radius of the grafting surface. Both trends reflect stronger crowding of dendrons in a quasi-planar brush than in a starlike DSPB.

Substitution of the equations for H, (13) and (14), into (8) gives the scaling expression of F_{conf}, which, because of a balance between the conformational entropy losses and the free energy of the monomer units repulsions, coincides (in scaling terms) with the total free energy F of a dendron in the brush. For $R_0 \gg H$ we obtain

$$\frac{F_+}{kT} \cong N(\sigma v)^{2/3}\left(\frac{N}{\mathcal{N}}\right)^{\beta/3}$$

$$\frac{F_\theta}{kT} \cong N\sigma w^{1/2}\left(\frac{N}{\mathcal{N}}\right)^{\beta/8} \tag{15}$$

and for $R_0 \ll H$

$$\frac{F_+}{kT} \cong N^{1/5}(fv)^{2/5}\left(\frac{N}{\mathcal{N}}\right)^{3\beta/5}$$

$$\frac{F_\theta}{kT} \cong (f^2w)^{1/4}\left(\frac{N}{\mathcal{N}}\right)^{3\beta/4} \tag{16}$$

Note that the total free energy of a dendron composed of N segments grows with the degree of branching, $N/\mathcal{N}$, according to power law, and the exponent is proportional to the parameter β. Thus, the free energy of a dendron in the brush is minimal for the first stretching model, i.e., the stretching of only one longest path in the dendrons (6), which corresponds to $\beta = 1$.

4. NUMERICAL SCF MODELING OF DSPB

4.1. Scheutjens–Fleer SCF Approach. Numerical SCF theory enables us to get more detailed and valuable insight into conformations of dendrons forming DSPB. The numerical SCF approach is based on the algorithm developed by Scheutjens and Fleer.[31] This approach uses a lattice which facilitates to account for the volume of all molecular components. According to the symmetry of the problem under consideration, the lattice sites are organized in spherical layers; each layer is referred to with a radial coordinate R (distance from the center of the lattice). Within a layer (along angular θ and ϕ coordinates), a mean-field approximation is applied; i.e., the volume fractions

dx.doi.org/10.1021/ma302632b | Macromolecules 2013, 46, 4651−4662

of the monomeric components and the self-consistent potential within the layer are constant, and angular fluctuations of these quantities are ignored. The presence of an impenetrable grafting spherical surface of the radius R_0 specifies the boundary condition: only the layers with $R > R_0$ are available for polymer and solvent molecules.

Many details of the SF-SCF method are readily available in the literature.[31] For the details of the SF-SCF calculations in the particular case of polymers with some branched topology see, for example, ref 30. Applications of the SF-SCF approach to planar dendritic polymer brushes were presented in refs 3 and 5.

The calculations were performed using the SFBox program developed in Wageningen University. The program outputs the local structural properties of DSPB (volume fraction distributions, $c_i(R)$, of all the segments of various types i, including terminal and branching points) which allow obtaining various integral properties (for example, the average thickness of the brush), without any preassumptions concerning distributions of the end points and branching points in the dendrons.

The volume fraction distributions can be easily converted into distributions $n_i(R)$ of the number of monomers of the type i in the spherical layer R. It is obtained by multiplying the volume fraction in the layer R by the number of lattice sites in the corresponding spherical layer $L(R)$, which is the volume of the spherical layer:

$$n_i(R) = c_i(R)L(R) \tag{17}$$

The volume of spherical layer is given by

$$L(R) = 4\pi(R^2 - R + 1/3) \tag{18}$$

The use of number distributions is the best way for expressing and analyzing the distribution of the branching and end points. On the other hand, number distributions are used for calculating averages of various conformational characteristics of the system under study.

To facilitate the comparison of DSPB (and LSPB) with different grafting densities, it is convenient to normalize the number distributions to unity by dividing them by number of grafted dendrons f and by the number m_i of monomers of the type i in a dendron

$$\frac{n_i(R)}{fm_i} \rightarrow n_i(R) \tag{19}$$

(for example, for branching points $m_{b1} = 1$, $m_{b2} = q$, $m_{b2} = q^2$, etc., for end groups $m_e = q^g$). Then

$$\sum_R n_i(R) = 1, \quad i = b1, b2, ..., e \tag{20}$$

The solvent is assumed to be good (athermal) for monomer units; hence, the Flory–Huggins interaction parameter is equal to zero: $\chi = 0$.

In order to mimic relevant experimental system and, at the same time, to unravel the main specific features arising from the topology of the end-grafted dendrons, in sections 4.2 and 4.3 we model the DSPB formed by the $g = 2$ generation dendrons with the functionality $q = 3$ (see Figure 1). Such a dendrons have the ratio $N/\mathcal{N} \approx 4.3$. We compare their structural properties to those of LSPB formed by linear chains with the same degree of polymerization N and the same grafting density σ. The spacer length in the dendrons is fixed at $n = 50$. We remark that this value is larger than that appeared usually in the experimental systems. However, this choice of the spacer length has enabled us to avoid artifacts arising in numerical SCF calculations for short chains and to improve the "resolution power" of the method. In section 4.4 we study the influence of the grafting density and the degree of branching on DSPB properties in detail.

4.2. Polymer Volume Fraction Profiles: Good Solvent Conditions. The polymer volume fraction profiles in DSPB and LSPB grafted with the same grafting density $\sigma = 0.1$ onto the surface of spherical particles with different curvature radii R_0 are presented in Figures 2a and 2b, respectively. The limiting

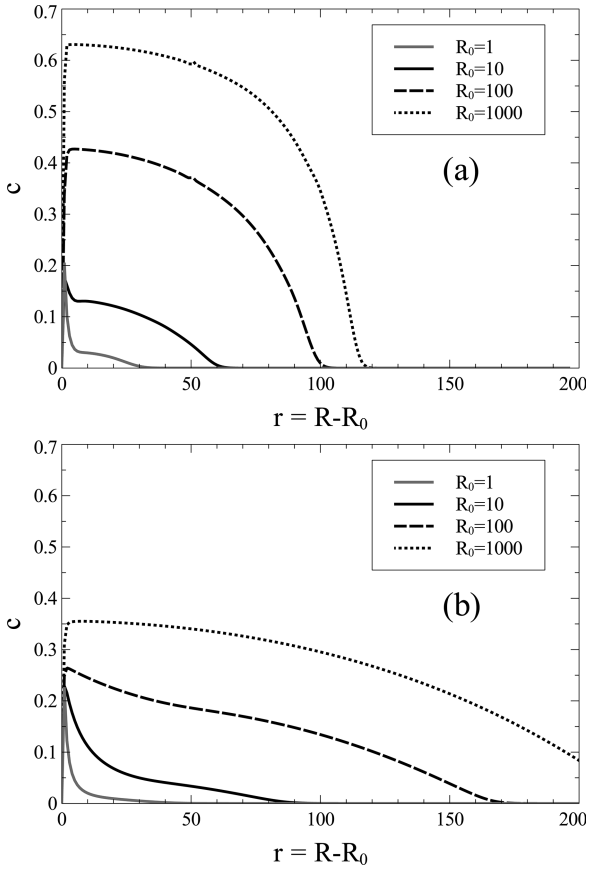

Figure 2. Polymer volume fraction profiles of DSPB with $g = 2$, $q = 3$, $n = 50$ (a) and LSPB (b) with the same degree of polymerization, $N = 650$, grafted to the core particle with radius R_0 at the same grafting density $\sigma = 0.1$. r is the radial distance from the grafting surface. The number of molecules in the brush, f, changes with R_0, and for a given set of R_0 equals $f = 3$, 139, 1.3×10^4, and 1.3×10^6.

cases of $R_0 = 1 \ll H$ (starlike brush) and $R_0 = 10^3 \gg H$ (quasi-planar brush) as well as the intermediate case of $R_0 \cong H$ are shown in Figure 2. Since the grafting density σ or, equivalently, the surface area per chain is kept constant, $s = 1/\sigma = 4\pi R_0^2/f$, different values of R_0 correspond to different total number, $f = 4\pi R_0^2/s$, of grafted molecules in the brush. The polymerization degree (the number N of monomer units) is taken the same in dendrons forming the DSPB and in linear chain forming the LSPB. The solvent is good (athermal), that is, the Flory–Huggins interaction parameter $\chi = 0$.

Comparison of the polymer volume fraction profiles presented in Figures 2a and 2b indicates that at any R_0 the height of the DSPB is always noticeably lower than that of LSPB formed by linear chains with the same degree of

dx.doi.org/10.1021/ma302632b | Macromolecules 2013, 46, 4651–4662

polymerization grafted at the same density. There are also differences in the internal structure of the brushes, i.e. in the shape of the volume fraction profiles, most pronounced at small curvature radius of the surface: In the starlike limit, the volume fraction profile in LSPB has a concave shape; the polymer volume fraction falls off sharply with distance from the grafting surface. It can be well approximated by a power law dependence $c(R) \sim R^{-4/3}$ corresponding to good solvent conditions.[12−15] With an increase in the curvature radius of the grafting surface, when $R_0 \cong H$, the volume fraction profile acquires a sigmoidal shape, one can clearly distinguish two regions: In the interior of the brush the volume fraction profile is still concave and can be approximated by a power law decay. The peripheral part of the volume fraction profile is convex and approaches the parabolic shape typical for a planar polymer brush.[22−25] At $R_0 \gg H$ a typical structure of the planar polymer brush with parabolically decaying polymer volume fraction, $c(r) \approx c(R_0)[1 - r^2/H^2]$, is recovered.

On the contrary, the volume fraction profile in DSPB at $R_0 \ll H$ has a convex shape with a peak near the grafting surface. An increase in the surface curvature radius does not lead to a qualitative change in the shape of the volume fraction profile for DSPB: It remains convex and progressively flattens off in the central region and decreases more sharply at the edge of the brush. A similar plateau-like polymer volume fraction profile has been found in SCF calculations for a single dendrimer molecule[30] (which mimics DSPB with $R_0 \ll H$, $f = q + 1$); the width of the region of constant polymer volume fraction increases upon an increase in the number of generations in the dendrimer.

Remarkably, for both LSPB and DSPB the overall thickness is an increasing function of the curvature radius R_0 (Figure 2). In Figure 3 the dependencies of DSPB and LSPB brush thicknesses on R_0 are shown. As a measure of the thickness we use the square root of the second moment of the polymer volume fraction distribution (rms distance between grafting surface and all of the brush monomer units) given by the formula

$$H = \left(\frac{\sum_{R>R_0} (R - R_0)^2 c(R) L(R)}{\sum_{R>R_0} c(R) L(R)} \right)^{1/2} \quad (21)$$

where the summation runs over all spherical layers R and $L(R)$ is given by eq 18. (In the case of uniform distribution of polymer volume fraction within the brush the value of H defined by eq 18 equals half of the total brush thickness.) We remind the reader that the grafting density and the degrees of polymerization of linear polymers and dendrons in LSPB and DSPB are the same. It can be seen that thicknesses of both DSPB and LSPB grow with R_0 and level off at $R_0 \gg H$. The inset in Figure 3 shows the ratio of thicknesses of both brushes, H_d/H_l, as a function of R_0. Here we see that this value decays while R_0 grows varying from 0.71 to 0.55.

We return to the comparison of the scaling formulas with the results of the SCF calculation in section 4.4.

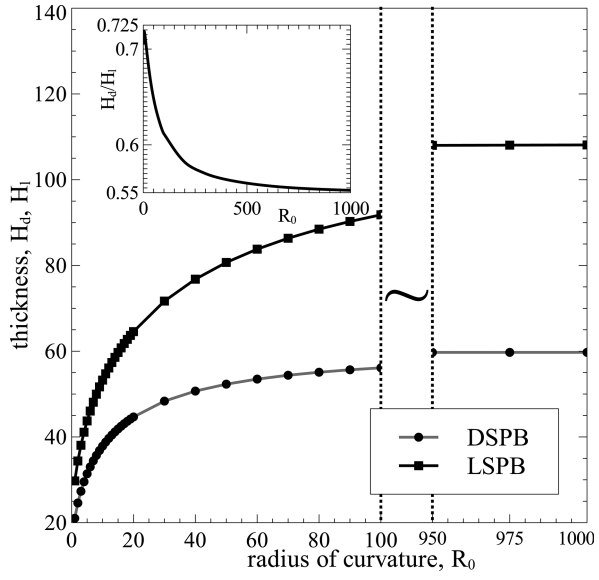

Figure 3. Dependence of the average thickness of LSPB and DSPB on the curvature radius R_0 of the grafting surface. The value of the thickness $H_{d,l}$ is the rms distance between grafting surface and all of the brush monomers, eq 21. Parameters of the brushes are introduced in the legend to Figure 2. The inset shows the ratio of DSPB and LSPB thicknesses H_d/H_l.

4.3. End Segments and Branching Points Distributions. The radial distributions of the branching points (in DSPB) and that of the end segments (in DSPB and LSPB) are presented in Figure 4 for different values of the curvature radius R_0. The analysis of these distributions points to different character of fluctuations of individual chains' extension in LSPB and DSPB at any curvature radius of the grafting surface.

The distribution of the free ends in the starlike LSPB ($R_0 \ll H$ which corresponds to the cases R_0 = 1, 10, and even 100) is peaked close to the periphery of the brush. As R_0 grows, the position of the maximum shifts to the right which corresponds to increasing thickness of the brush (see Figure 3). Importantly, there is a "dead zone" in the region close to the grafting surface where no free ends of the chains are found. This "dead zone" approximately corresponds to the range of R where the polymer volume fraction decay is well approximated by a power law function (see Figure 2b).

The end monomers distribution in starlike DSPB also exhibits a single maximum when R_0 = 1 and 10. However, in contrast to LSPB, no "dead zone" for chain ends in the central region of the brush is found. Note that the SCF analysis of the end-segment distribution in a dendrimer[30] pointed out to a similar wide unimodal (with one pronounced maximum) distribution of the end-points: in the dendrimer as well as in the starlike DSPB, the polymer volume fraction decreases weakly (following nonpower law function) as a function of the radial distance from the center due to increasing number of branches in outer generations. This behavior is similar to fluctuations of linear chains in a planar polymer brush,[22−25] where the polymer volume fraction decreases as a nonpower law function of the distance from the grafting surface and the free ends are distributed (with a broad maximum) throughout the brush.

Distribution function of the branching points at R_0 = 1 and 10 are also unimodal. With an increase in R_0 they shift to the right. If we assume that the position of the maximum of the corresponding distribution approximately coincides with its average, than we can estimate a stretching degree of a spacers of each generations as r^{b1}_{max}/n for the root spacers, $(r^{b2}_{max} - r^{b1}_{max})/n$ for the spacers belonging to the first generation, and $(r^{e}_{max} - r^{b2}_{max})/n$ for the third generation (terminal) spacers. As is seen from Figures 4a and 4b the stretching degree of spacers decreases with increasing the generation number. Spacers of the

dx.doi.org/10.1021/ma302632b | Macromolecules 2013, 46, 4651−4662

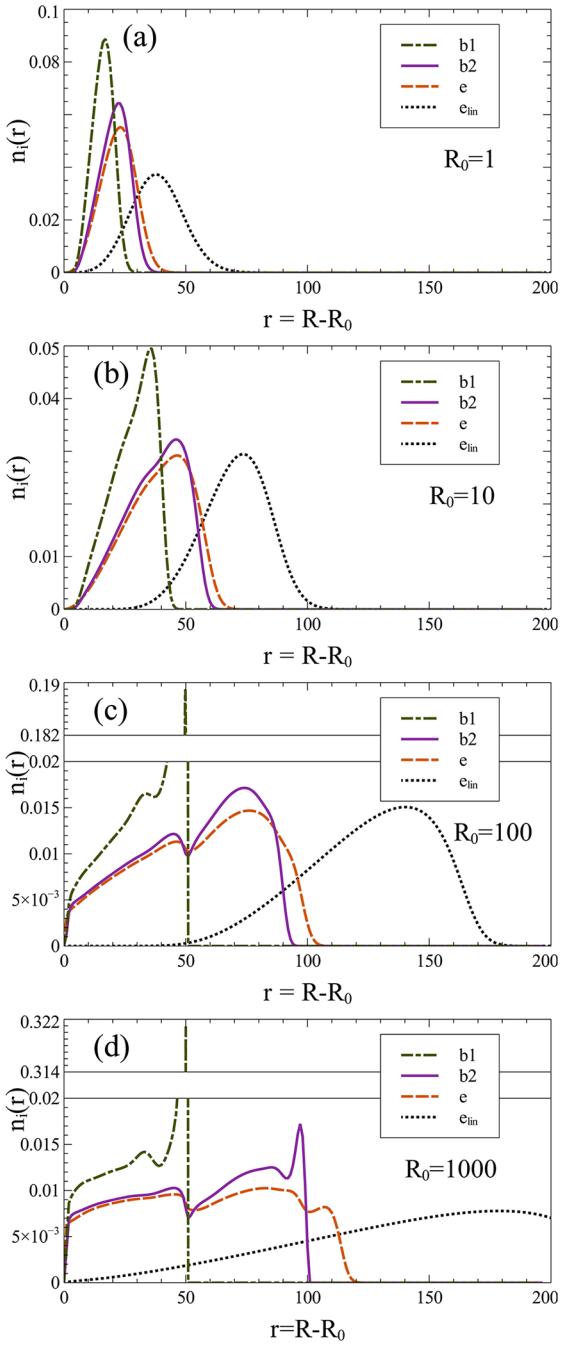

Figure 4. Probability distribution of branching, $b1$ and $b2$, and terminal, e, segments of dendritic brush and the distribution of terminal segments of a linear brush, e_{lin}, given for different curvature radii R_0 = 1 (a), R_0 = 10 (b), R_0 = 100 (c), and R_0 = 1000 (d). Parameters of the brushes are introduced in the legend to Figure 2. These distributions are normalized in such a way that the area below each curve equals unity.

second generations (terminal spacers) are almost unstretched at R_0 = 1 and 10.

Further increase in the curvature radius of the grafting sphere leads to transformations of the end-segment distributions, in both LSPB and DSPB, and of branching segments distribution in DSPB. In LSPB the end-point distribution remains unimodal, but the maximum becomes broader, and at R_0 = 1000 the "dead zone" near the grafting surface disappears. In the $R_0 \gg H$ limit a typical for a planar polymer brush distribution $c_{end}(r) \sim r[1 - r^2/H^2]^{1/2}$ [22−25] is observed.

On the contrary, the unimodal distributions observed at R_0 = 1 and 10 in DSPB completelly change their shape when $R_0 \simeq H$ and $R_0 \gg H$, getting similar to that of a planar dendritic brush.[3,5] In the limiting case, R_0 = 1000, the distribution function of the first branching point ($b1$) has two maxima; the right one corresponds to almost completely stretched root spacers. The distribution function of the second branching point ($b2$) has three maxima where the rightmost one corresponds to completely stretched both root and first-genetarion spacers.

The distribution of terminal groups also has three maxima. The rightmost maximum of the end distribution (e) in Figure 4c,d corresponds to the population of strongly stretched dendrons, whose ends are located close to the edge of the brush. This "extended" population gets noticeably enriched upon an increase in R_0. The leftmost and the middle maxima of ends distribution correspond to the population of weakly and moderately extended dendrons; they remain relatively wide in the whole range of $r = R - R_0$.

As it has been shown in refs 3 and 5 for planar dendritic brushes, such highly pronounced multimodal distributions of end and branching points signify the intrabrush segregation of dendrons. On the basis of the model suggested in refs 3 and 5 one can explain such a complicated behavior as follows: First, when the curvature is high, R_0 = 1 and 10 (Figure 4a, b), we see only one population of the weakly stretched dendrons, with unimodal distributions of branching and end points. Such a case is schematically shown in Figure 5a. Next, when the curvature decreases, at R_0 = 100, the second population of dendrons with completelly stretched root spacers emerges, and this is manifested by a sharp peak in the $b1$ distribution near to r = 50 (Figure 4c). The remaining dendrons (of the first population) fill the space between the grafting surface and the position of this peak. Dendrons of the second population are located entirely (exept the root spacer) above the first population ones. One can treat it as the next layer dendron brush with one generation less (see Figure 5b). Finally, when the brush is almost planar, at R_0 = 1000 (Figure 4d), the third population of dendrons emerges. Dendrons belonging to this population have a fully extended root spacer and the first generation spacers as well, as indicated by pronounced maxima of $b1$ and $b2$ distributions at r = 50 and r = 100, respectively. The remaining terminal spacers of the third generation dendrons might be treated as the third layer *linear* brush (Figure 5c). The three polpulations of dendrons coexist in dynamic equilibrium in the brush. This multimodal distribution of extension of dendrons in planar dendritic brushes is caused by the finite extensibility of spacers and ensures packing of the monomer units inside the brush with virtually constant polymer volume fraction.[3−5]

4.4. Scaling Relations: Proof by the SCF Approach. In section 3.2, scaling dependencies for the DSPB thickness (eqs 13, 14) and the average polymer volume fraction in DSPB (eqs 11, 12) on the degree of branching ($N/\mathcal{N}$) and the grafting density σ or the ratio f/N^2 were derived for limiting cases $R_0 \gg H$ (quasi-planar brush) and $R_0 \ll H$ (starlike brush) in the framework of the simple boxlike model. The SF-SCF approach permits obtaining more detailed information about the structural organization of DSPB for various R_0, grafting densities, and degrees of branching.

dx.doi.org/10.1021/ma302632b | *Macromolecules* 2013, 46, 4651−4662

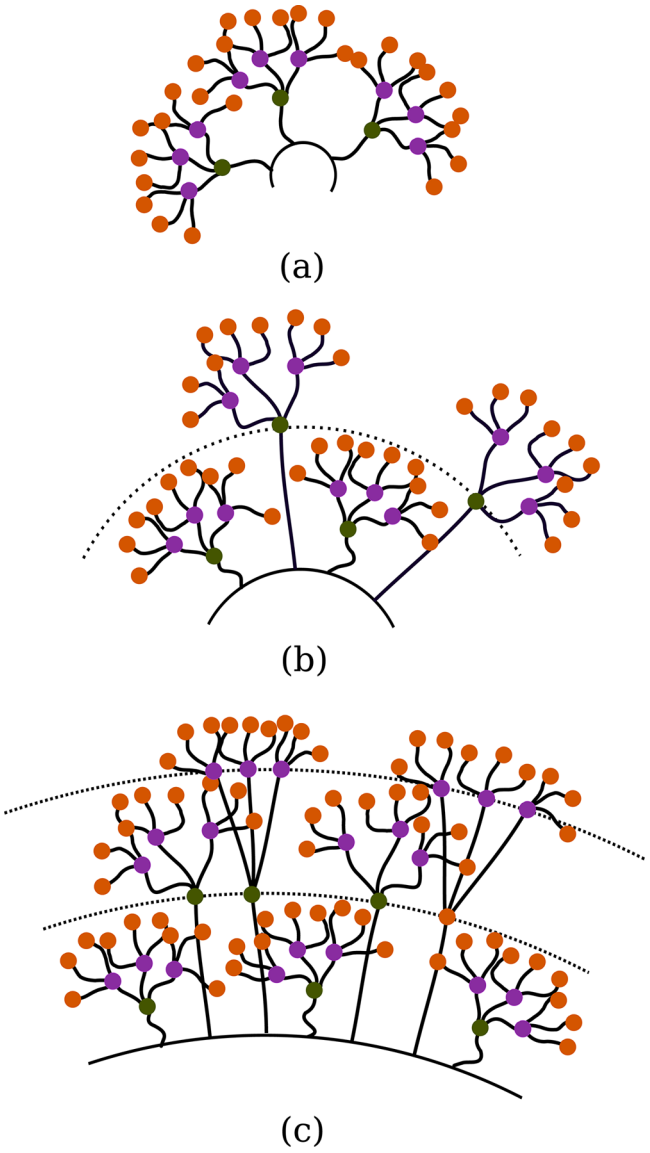

Figure 5. A multilayer and multistretching structure manifests itself more and more as the curvature decreases.

In the section 4.2 the mean-square brush height H was calculated from the polymer volume fraction profiles in DSPB and LSPB obtained by the SF-SCF method for various R_0 (see Figure 3). In the inset to Figure 3 the ratio of the DSPB and the LSPB heights as a function of R_0 is presented. (We recall that dendrons and linear chains forming DSPB and LSPB, respectively, have the same molecular weight and are grafted at the density $\sigma = 0.1$.) As it follows from eqs 13 and 14, in the starlike brush, $R_0 \ll H$, the ratio H_d/H_l should assume the values between $(N/\mathcal{N})^{-1/5}$ and $(N/\mathcal{N})^{-2/5}$, whereas for quasi-planar brush, $R_0 \gg H$, the ratio H_d/H_l should be found between $(N/\mathcal{N})^{-1/3}$ and $(N/\mathcal{N})^{-2/3}$. A DSPB considered in Figure 3 is formed by second generation dendrons, $g = 2$, with the functionality $q = 3$, so that $(N/\mathcal{N}) = 4.3$. Hence, the value of the ratio H_d/H_l on the left boundary of Figure 3 (starlike case, $R_0 \ll H$) must fall into the interval 0.56−0.74, whereas on the right boundary (quasi-planar case, $R_0 \gg H$) it is expected to assume the value in the range 0.38−0.61. It can be seen that the obtained from the SCF calculation values 0.71 at $R_0 = 1$ and 0.55 at $R_0 = 1000$ are found within the predicted by scaling estimates interval and are closer to the upper limit corresponding to the value of $\beta = 1$ in eqs 13 and 14. We recall that the value $\beta = 1$ corresponds to the particular distribution of strain in the dendrons (the longest elastic path extension mode).

In order to further analyze the mode of the dendrons deformation in DSPB, we have performed the SF-SCF calculations of the volume fraction profiles in planar and starlike DSPB at various grafting densities and degrees of branching. We examined scaling dependencies of the average polymer volume fraction in the brush which can be calculated from the volume fraction profile as

$$\langle c \rangle = \frac{\sum_{R>R_0} c(R)^2 L(R)}{\sum_{R>R_0} c(R) L(R)} \tag{22}$$

where the summation runs over all the layers R.

Let us begin from the quasi-planar brush case and consider dependences of $\langle c \rangle$ on σ and $N/\mathcal{N}$. In the quasi-planar limit, the boxlike model predicts the scaling dependence $c \sim \sigma^{2/3}$ under good solvent conditions, both for linear and dendritic brushes (eq 11). To check this prediction, Figure 6 shows

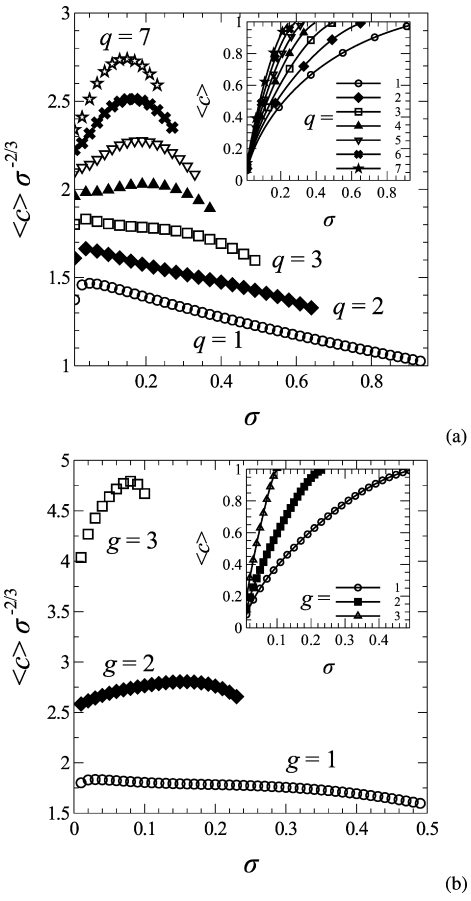

Figure 6. Dependencies of the average polymer volume fraction in planar dendritic brushes on the grafting density σ calculated for (a) first-generation dendrons brush, $g = 1$, and various functionalities, q, of the branching point and (b) brushes made by dendrons of various generations, g, with the same functionality, $q = 2$, of branching points. The main panels show the dependencies of the scaled product $\langle c \rangle \sigma^{-2/3}$ on σ, whereas the dependencies for the nonscaled volume fraction $\langle c(\sigma) \rangle$ are given in the insets.

dx.doi.org/10.1021/ma302632b | Macromolecules 2013, 46, 4651−4662

dependencies of the rescaled average polymer volume fraction $\langle c\rangle\sigma^{-2/3}$ on the grafting density σ at $R_0 \gg H$ (the "original" $\langle c(\sigma)\rangle$ dependencies are given in the insets). According to scaling, the product $c\sigma^{-2/3}$ must be invariant with respect to σ (provided that other parameters of the brush are fixed). However, as one can see in Figure 6 there are deviations from the scaling predictions in the considered range of σ values. For brushes made of linear chains (q = 1, panel a) and for dendritic brushes with low branching functionality q and number of generations g an increase in grafting density σ leads to a weaker increase in the polymer volume fraction $\langle c\rangle$ as a function of σ compared to scaling prediction.

An increase in the degree of branching $N/\mathcal{N}$ (an increase in q, Figure 6a, or in g, Figure 6b) changes the character of the dependence of $\langle c\rangle\sigma^{-2/3}$ on σ. It becomes nonmonotonic; the product $\langle c\rangle\sigma^{-2/3}$ first grows and after passing through a maximum decreases as a function of σ. We recall that the scaling consideration, section 3.2, is based on the assumption of low polymer volume fraction in the brush and not too strong stretching of the chains as well. This allowed us to consider only two-body monomer−monomer interactions (in the case of a good solvent) and to assume Gaussian chain elasticity.

One can suggest that a decrease in $\langle c\rangle\sigma^{-2/3}$ with increasing σ is caused by increasing importance of the third and higher order repulsive interactions, whereas the initial growth of $\langle c\rangle\sigma^{-2/3}$ as a function of σ is a consequence of the limited extensibility (nonlinear elasticity) of the dendron spacers. As it is seen from Figure 4 for quasi-planar DSPB with $N/\mathcal{N}$ = 4.3 and σ = 0.1 there is a noticeable number of extremely stretched spacers. Data from Figure 6a,b show that the effect of limited extensibility begins to manifest itself at $N/\mathcal{N} \geqslant 3$.

Consider now the dependence of $\langle c\rangle$ on the degree of branching $N/\mathcal{N}$. Figure 7 presents logarithmic dependences of

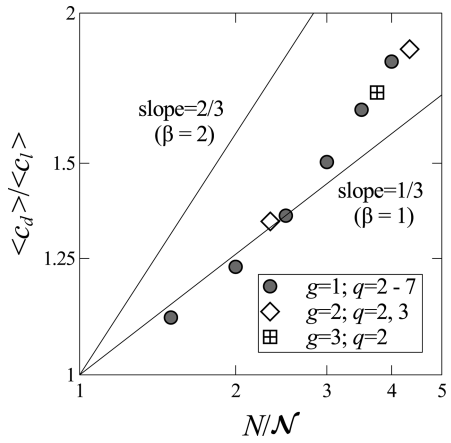

Figure 7. Dependencies of dendritic-to-linear brush mean volume fraction ratio on the degree of branching $N/\mathcal{N}$ in first- to third generation brush, g = 1−3, of various functionalities q as indicated, σ = 0.1.

$\langle c_d\rangle/\langle c_l\rangle$ on $N/\mathcal{N}$ compared with the "boundary dependencies" $(N/\mathcal{N})^{1/3}$ and $(N/\mathcal{N})^{2/3}$ following from eq 11. We remark that the straight lines describing these boundary dependences cross at the origin since by definition $\langle c_d\rangle/\langle c_l\rangle$ = 1 at $N/\mathcal{N}$ = 1. It can be seen that the results of SCF modeling are grouped around the predicted lower volume fraction limit, i.e., correspond to minimal free energy penalty in DSPB (β = 1). This result is in a line with conclusion, which follows from the analysis of the ratio between thicknesses of LSPB and DSPB with g = 2 and q = 3 (Figure 3).

Let us now check the validity of scaling predictions for the starlike DSPB, $R_0 \ll H$. Figure 8 presents dependencies of the

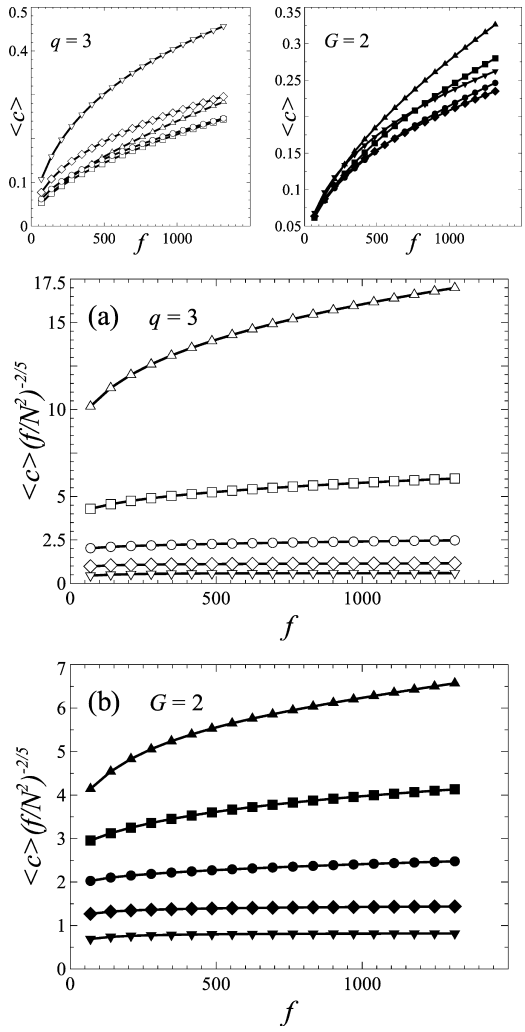

Figure 8. Dependences of average polymer volume fraction in starlike (R_0 = 10) dendritic brushes on the number of dendrons f (two top panels). Two bottom panels, (a) and (b), show dependencies of the scaled product $\langle c\rangle$ $(f/N^2)^{-2/5}$ on f. In panel (a) these dependencies are given for constant q = 3 and various g. Panel (b) includes the cases of constant g = 2 and various q. The correspondence between each curve in the panels and a particular pair (g, q) is given in Table 1.

average polymer volume fraction $\langle c\rangle$ and its rescaled value $\langle c\rangle(f/N^2)^{-2/5}$ on the number f of dendrons in a brush grafted onto a spherical particle with the radius R_0 = 10. Similarly to the planar brush case, two modes of varying the degree of branching $N/\mathcal{N}$ (by changing either q or g) are represented. The correspondence of each curve to particular (f, g) pair are given in Table 1, where the respective degree of dendron branching, $N/\mathcal{N}$, is also indicated.

It can be seen that for starlike DSPB with not too high values of $N/\mathcal{N}$ the rescaled average polymer volume fraction, $\langle c\rangle(f/N^2)^{-2/5}$, remains almost constant, which is in agreement with eq 12. Only for $N/\mathcal{N} \geqslant 5$ the deviations from the scaling dependence in the direction of increasing $\langle c\rangle$ with increase in f are observed. This is a manifestation of a limited spacers extensibility. Note that in this study the spherical symmetry of

dx.doi.org/10.1021/ma302632b | Macromolecules 2013, 46, 4651−4662

Table 1. Degree of Dendron Branching $N/\mathcal{N}$ Depending on Its Generation, g, and Functionality, q

symbol	g	q	$N/\mathcal{N}$	symbol	g	q	$N/\mathcal{N}$
▽	0	3	1.0	▼	2	1	1.0
◇	1	3	2.0	◆	2	2	2.3
○	2	3	4.3	●	2	3	4.3
□	3	3	10.0	■	2	4	7.0
△	4	3	24.2	▲	2	5	10.3

the system leads to a smaller value of $\langle c\rangle$ in DSPB compared with planar brushes (cf. Figures 6a,b and 8a,b). Therefore, the interactions of orders higher than the second do not significantly affect the $\langle c\rangle$, so that a decrease in $\langle c\rangle(f/N^2)^{-2/5}$ upon an increase in f is not observed.

Figure 9 shows (in a log−log scale) the ratio $\langle c_d\rangle/\langle c_l\rangle$ of average polymer volume fractions in DSPB and LSPB with the same grafting density, $\sigma = 0.1$, the curvature radius, $R_0 = 10$, and the molecular weight, N, at different degrees of branching in DSPB, $N/\mathcal{N}$. It is seen that the obtained by SF-SCF values of this ratio lie near the lower boundary of its possible range, which is estimated in section 3.2, eq 12 at $\beta = 1$. Note, however, that these values fall even below the estimated permissible range that may be a consequence of use of the simplified model of LSPB and DSPB for derivation of scaling relations. Note also that with increasing $N/\mathcal{N}$ in Figure 9 the ratio $\langle c_d\rangle/\langle c_l\rangle$ deviates upward from the lower border (corresponding to $\beta = 1$). That is the same effect which was observed in the case of planar brushes (Figure 7). It is associated with a non-Gaussian elasticity of spacers in highly branched dendrons.

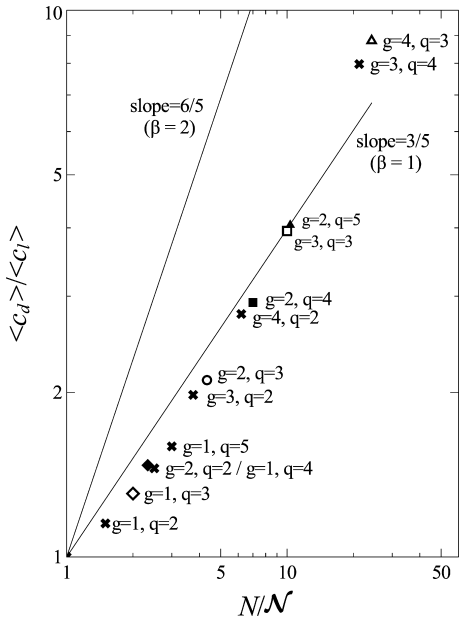

Figure 9. Dependence of dendritic-to-linear brush mean volume fraction ratio on the degree of branching $N/\mathcal{N}$ for starlike dendritic brushes ($R_0 = 10$) composed by dendrons with various functionalities, q, and generations, g. Combinations of q and g are in accordance with Table 1. Pairs (q, g) not included in Table 1 are marked with crosses.

In general, comparison of the results of SF-SCF calculations and scaling estimates for the two geometries of dendritic brushes, i.e., planar, $R_0 \gg H$, and starlike, $R_0 \ll H$, shows that in the considered here (and experimentally most relevant) range of $N/\mathcal{N}$ the structure of DSPB is better described by model of the "longest path" stretching, corresponding to the case $\beta = 1$ in eq 8. The deviation between the results of caclulations and single-power law dependences of the reduced polymer volume fraction observed in Figures 7 and 9 for large values of the branching parameter $N/\mathcal{N}$ might be attributed to manifestation of finite extensibility (non-Gaussian elasticity) of the spacers. Now let us discuss in detail the mechanism of the dendrons deformation in a brush at $\beta = 1$.

4.5. Dendrons Deformation in DSPB. The above analysis of the brush properties obtained by the SF-SCF calculations indicates that the conformations of dendrons in DSPB approximately correspond to the stretching mode with minimal entropy losses, i.e., $\beta = 1$ in eqs 8−10.

This limiting scenario is equivalent to stretching of only one spacer within each generation ("longest path" stretching model). At the same time the direct MD simulation of the planar brush of dendrons[4] does not provide a clear evidence of stretching of one ("selected") spacer per each generation. This contradiction between theory and simulations is, however, only apparent.

The idea of of a single spacer extension per each generation was introduced[3] in order to estimate the minimum entropy losses upon the dendron stretching. However, eq 6 allows for a different interpretation, which is closer to the simulation results.[3−5] Let us rewrite (6) in the form

$$\frac{F_{\mathrm{conf}}^{(\min)}}{k_{\mathrm{B}}T} \cong \mathcal{N}\frac{H^2}{\mathcal{N}^2} = \mathcal{N}\alpha^2 = n(g+1)\alpha^2 \tag{23}$$

where $\alpha = H/\mathcal{N}$ is the overall degree of stretching of a dendron. Hence, the contribution of each generation to the overall stretching free energy does not depend on the generaton number and is equal to

$$\left(\frac{F_{\mathrm{conf}}^{(\min)}}{k_{\mathrm{B}}T}\right)_g \cong n\alpha^2 \tag{24}$$

The number of spacers in the generation g is equal to q^g; therefore, the average contribution of each spacer to $F_{\mathrm{conf}}^{(\min)}$ is

$$\frac{1}{q^g}\left(\frac{F_{\mathrm{conf}}^{(\min)}}{k_{\mathrm{B}}T}\right)_g \cong \frac{n\alpha^2}{q^g} = n{\alpha_{\mathrm{eff}}}^2 \tag{25}$$

where $\alpha_{\mathrm{eff}} = \alpha q^{-g/2}$ is the average degree of spacer's extension in the generation g. Thus, the average extension of spacers in each generation decreases in this scenario as a function of ranking number of generation. Such a decay in extension of a spacer have been studied in detail in ref 5.

We emphasize that the above mode of dendrons stretching in a brush leading to $\beta = 1$ corresponds to the minimum free energy of the brush eq 3. Therefore, the manifestation of such a mode of the dendrons stretching in the brush is not surprising.

5. DISCUSSION AND CONCLUSIONS

We have presented a scaling theory of conformations of regularly branched macromolecules (dendrons) grafted to the surfaces of arbitrary curvature and complemented the scaling analysis by molecular realistic assumption-free numerical SCF modeling. As limiting cases, our theory describes equilibrium structure of planar dendritic brush ($R_0 \to \infty$) and regular starburst polymers ($R_0 \to 0$). As we have demonstrated, the effect of the branched topology of individual macromolecules

dx.doi.org/10.1021/ma302632b | Macromolecules 2013, 46, 4651−4662

forming the brush on the integral structural properties of the brush can be accounted for by using the universal scaling parameter $N/\mathcal{N} \geq 1$, where $\mathcal{N}$ is the number of monomer units in the longest elastic path in a dendron. In the limit $N/\mathcal{N} = 1$ the properties of the brushes formed by end-grafted linear polymers are recovered. We anticipate that scaling relation derived in the present work are applicable for brushes formed by *regularly* branched macromolecules of arbitrary topology (star-like, dendrons, comb-shape, etc.) where the value of exponent β may vary in the range from unity to two, depending on the particular topology and also on the grafting density.

The major limitation of the scaling approach in application to DSPB is related to significantly higher volume fraction of monomer units inside the brush as compared to that in LSPB. Indeed, when the volume fraction of polymer inside the brush exceeds a few tens of percent, the contribution of binary, ternary, and higher order interactions to the free energy are comparable. Hence, the range of applicability of the power law dependences of the brush thickness on grafting density corresponding to good or theta-solvent conditions are narrow and overlap with the crossover regimes.

As follows from our SCF results, in both LSPB and DSPB a variation of the ratio of the surface curvature radius R_0 to the characteristic brush thickness H affects not only the shape of the polymer volume fraction profile but also the character of fluctuations in extension of individual macromolecules forming the brush: In LSPB the polymer volume fraction decreases as a power-law function of a distance from the center of curvature, and the chain ends distribution is peaked near the edge of the brush at small $R_0/H \ll 1$, whereas at large $R_0/H \gg 1$ the polymer volume fraction decay is weaker and the chain ends are distributed throughout the brush. In contrast, in DSPB the polymer volume fraction distribution is fairly uniform irrespectively of the ratio R_0/H. This uniform volume fraction distribution is assured by fairly uniform distribution of the end segments throughout the brush at $R_0/H \ll 1$ or by multimodal distribution of the overall extension of dendrons at $R_0/H \gg 1$. Hence, we can conclude that availability of possibly functionalized end groups in DSPB decreases upon an increase in the curvature radius of the surface.

In refs 8 and 9 a detailed comparison of experimentally accessible structural properties of LSPB and DSPB was performed. Linear or dendritically branched macromolecules with approximately the same molecular weight (2737 and 2477 Da, respectively) were grafted to SPIONs with an average diameter 7.33 nm. The dimensions of the "core" nanoparticles was smaller than the overall hydrodynamic diameter (measured by DLS) of the resulting SPB, which enables direct comparison of the experimental results to the predictions of the scaling theory for SPBs in the starlike limit, $R_0 \ll H$. The hydrodynamic thickness of the brush, calculated as a difference between measured in the DLS expriments hydrodynamic radius of the brush and radius of the core SPION, was $H_l \approx 7.84$ nm and $H_d \approx 4.84$ nm for LSPB and DSPB, respectively. The characteristic branching parameter for the dendrons forming DSPB could be estimated as $N/\mathcal{N} \approx 6$. Hence, the experimentally measured ratio H_d/H_l can be fitted by eq 14 under good solvent conditions with an apparent value of the exponent $\beta \approx 1.34$, which can be attributed to the crossover between two limiting stretching regimes. Hence, we can conclude that our scaling theory satisfactory describes the experimentally observed dependence of the DSPB thickness on the degree of branching of the brush-forming dendrons.

AUTHOR INFORMATION

Corresponding Author

*E-mail: helvrud@gmail.com (O.V.R.); oleg.borisov@univ-pau.fr (O.V.B.).

Notes

The authors declare no competing financial interest.

ACKNOWLEDGMENTS

This work has been partially supported within Scientific and Technological Cooperation Program Switzerland-Russia, project "Experimental studies and theoretical modelling of amphiphilic di/triblock and dendritic functional polymers at surfaces: influence of interfacial architecture on biological response", Grant Agreement No. 128308, by the Russian Foundation for Basic Research (Grants 11-03-00969a and 12-03-31243) and by Department of Chemistry and Material Science of the Russian Academy of Sciences.

REFERENCES

(1) Picket, G. T. *Macromolecules* **2001**, *34*, 8784.
(2) Kröger, M.; Peleg, O.; Halperin, A. *Macromolecules* **2010**, *43*, 6213.
(3) Polotsky, A. A.; Gillich, T.; Borisov, O. V.; Leermakers, F. A. M.; Textor, M.; Birshtein, T. M. *Macromolecules* **2010**, *43*, 9555.
(4) Merlitz, H.; Wu, C.-X.; Sommer, J.-U. *Macromolecules* **2011**, *44*, 7043−7049.
(5) Polotsky, A. A.; Leermakers, F. A. M.; Zhulina, E. B.; Birshtein, T. M. *Macromolecules* **2012**, *45*, 7260.
(6) Guo, Y.; van Beek, J. D.; Zhang, B.; Colussi, M.; Walde, P.; Zhang, A.; Kröger, M.; Halperin, A.; Schlüter, A. D. *J. Am. Chem. Soc.* **2009**, *131*, 11841.
(7) Borisov, O. V.; Zhulina, E. B.; Birshtein, T. M. *ACS Macro Lett.* **2012**, *1*, 1166.
(8) Gillich, T. Self-organization of Catechol-Functionalized Dendrons for the Creation of Non- Interactive, Antifouling Biointerfaces in 2D and 3D. PhD Thesis, ETH Zurich, 2011.
(9) Gillich, T.; Benetti, E. M.; Rakhmatullina, E.; Konradi, R.; Li, W.; Zhang, A.; Schlüter, A. D.; Textor, M. *J. Am. Chem. Soc.* **2011**, *133*, 10940.
(10) Ballauff, M. *Prog. Polym. Sci.* **2007**, *32*, 1135−1151.
(11) Aseyev, V. O.; Tenhu, H.; Winnik, F. M. *Adv. Polym. Sci.* **2011**, *242*, 29−89.
(12) Daoud, M.; Cotton, J.-P. *J. Phys. (Paris)* **1982**, *43*, 531.
(13) Zhulina, E. B. *Polym. Sci. USSR* **1984**, *26*, 794.
(14) Birshtein, T. M.; Zhulina, E. B. *Polymer* **1984**, *25*, 1453.
(15) Zhulina, E. B.; Birshtein, T. M.; Borisov, O. V. *Eur. Phys. J. E* **2006**, *20*, 243−256.
(16) Alexander, S. *J. Phys. (Paris)* **1977**, *38*, 983.
(17) de Gennes, P.-G. *Macromolecules* **1980**, *13*, 1069.
(18) Birshtein, T. M.; Zhulina, E. B. *Polym. Sci. USSR* **1983**, *A25*, 2165−2174.
(19) Birshtein, T. M.; Zhulina, E. B. *Polym. Sci. USSR* **1999**, *A41*, 2165−2174.
(20) Wijmans, C. M.; Zhulina, E. B. *Macromolecules* **1993**, *26*, 7214−7224.
(21) Birshtein, T. M.; Mercurieva, A. A.; Leermakers, F. A. M.; Rud, O. V. *Polym. Sci. USSR* **2008**, *A50*, 992.
(22) Skvortsov, A. M.; Pavlushkov, I. V.; Gorbunov, A. A.; Zhulina, E. B.; Borisov, O. V.; Pryamitsyn, V. A. *Polym. Sci. USSR* **1988**, *30*, 1706.
(23) Milner, S. T.; Witten, T. A.; Cates, M. *Macromolecules* **1988**, *21*, 2610.
(24) Zhulina, E. B.; Pryamitsyn, V. A.; Borisov, O. V. *Polym. Sci. USSR* **1989**, *31*, 205.
(25) Zhulina, E. B.; Borisov, O. V.; Pryamitsyn, V. A.; Birshtein, T. M. *Macromolecules* **1991**, *24*, 140.
(26) Ballauff, M.; Likos, C. *Angew. Chem., Int. Ed.* **2004**, *43*, 2998.

(27) de Gennes, P.-G.; Hervet, H. *J. Phys. (Paris)* **1983**, *44*, L351.
(28) Mansfield, M. L.; Klushin, L. I. *Macromolecules* **1993**, *26*, 4262.
(29) Boris, D.; Rubinstein, M. *Macromolecules* **1996**, *29*, 7251.
(30) Klein Wolterink, J.; van Male, J.; Daoud, M.; Borisov, O. V. *Macromolecules* **2003**, *36*, 6624.
(31) Fleer, G. J.; Cohen Stuart, M. A.; Scheutjens, J. M. H. M.; Cosgrove, T.; Vincent, B. *Polymers at Interfaces*; Chapman & Hall: London, 1993.